CONF-960457--6

Note: This is a preprint of paper being submitted for publication. Contents of this paper should not be quoted nor referred to without permission ot the author(s).

Submitted to:
International Conference on Metallurgical Coatings and Thin Films, Town and Country Hotel
San Diego, California
April 22–26, 1996

The Calculation of Thin Film Parameters from Spectroscopic Ellipsometry Data

G. E. Jellison, Jr.
Solid State Division
Oak Ridge National Laboratory
Oak Ridge, TN 37830

"The submitted manuscript has been authored by a contractor of the U.S. Government under contract DE-AC05-96OR22464. Accordingly, the U.S. Government retains a nonexclusive, royalty-free license to publish or reproduce the published form of this contribution, or allow others to do so, for U.S. Government purposes."

February 1996

Prepared by
Solid State Division
Oak Ridge National Laboratory
P.O. Box 2008
Oak Ridge, Tennessee 37831-6056
managed by
LOCKHEED MARTIN ENERGY SYSTEMS, INC.
for the
U.S. DEPARTMENT OF ENERGY
under contract DE-AC05-96OR22464

MASTER

DISTRIBUTION OF THIS DOCUMENT IS UNLIMITED

DISCLAIMER

Portions of this document may be illegible in electronic image products. Images are produced from the best available original document.

The Calculation of Thin Film Parameters from Spectroscopic Ellipsometry Data

G. E. Jellison, Jr.
Solid State Division
Oak Ridge National Laboratory
Oak Ridge, TN 37830

Abstract

Spectroscopic ellipsometry (SE) has proven to be a very powerful diagnostic for thin film characterization, but the results of SE experiments must first be compared with calculations to determine thin film parameters such as film thickness and optical functions. This process requires 4 steps: (1) The quantities measured must be specified and the equivalent calculated parameters identified. (2) The film structure must be modeled, where the number of films is specified and certain characteristics of each layer specified, such as whether or not the film is isotropic or anisotropic, homogeneous or graded. (3) The optical functions of each layer must be specified or parameterized. (4) The data must be compared with the calculated spectra, where a quantifiable figure of merit is used for the comparison. The last step is particularly important because without it, no "goodness of fit" parameter is calculated and one does not know whether or not the calculated spectrum fits the data.

DISCLAIMER

This report was prepared as an account of work sponsored by an agency of the United States Government. Neither the United States Government nor any agency thereof, nor any of their employees, makes any warranty, express or implied, or assumes any legal liability or responsibility for the accuracy, completeness, or usefulness of any information, apparatus, product, or process disclosed, or represents that its use would not infringe privately owned rights. Reference herein to any specific commercial product, process, or service by trade name, trademark, manufacturer, or otherwise does not necessarily constitute or imply its endorsement, recommendation, or favoring by the United States Government or any agency thereof. The views and opinions of authors expressed herein do not necessarily state or reflect those of the United States Government or any agency thereof.

I. Introduction

Spectroscopic ellipsometry (SE) has become increasingly important as a thin film diagnostic tool over the last decade [1]. Ellipsometry is a polarization-sensitive optical reflection technique [2], generally in the near ultraviolet–near infrared wavelength region, which means that it is non-destructive, and can be used in high-pressure and magnetic environments, situations where electron diagnostics cannot be used. However, the data obtained directly from SE measurements is usually not interesting; usable thin film parameters, such as film thickness, surface roughness, optical functions of the films, etc., must be obtained from the data by model calculations compared with the data. This is a common exercise in science and engineering, and as such is well understood.

This interpretation of SE data requires 4 steps (Ref. 3 discussed the last three). The first step is to determine the parameters that are measured. This will depend on the SE instrument used, on the configuration of optical elements within the instrument, and on the characteristics of the sample and other perturbing optics, such and vacuum chamber windows. The second step is to specify the way in which the Fresnel Reflection coefficients (FRCs) are calculated. If the sample consists of several homogeneous layers of isotropic materials, simple 2×2 matrix methods are appropriate; if one or more of the films are inhomogeneous (where the optical functions vary with film thickness) or anisotropic, more complicated 2×2 matrices or 4×4 matrices must be used. The third step is to specify the optical functions of each layer; this can be a specification of a data base spectrum, a parameterization of the optical functions, or a combination of the two. The fourth step is the comparison of the calculated Fresnel reflection coefficients with the experimental parameters; this is the critical step in that it determines the confidence one has concerning whether or not the calculation actually fits the data. In this paper, each of these four steps are reviewed.

II. Measured Parameters

A general schematic representation of a generalized SE instrument [2,4] is shown in Fig. 1. The light source produces a collimated light beam, which passes through a polarization state generator (PSG), reflects off the sample (S), passes through a polarization state detector (PSD) and is then detected. The monochromator can be either before the light enters the PSG or after it exits the PSD. The PSG and the PSD each consist of polarizers and/or compensating optical elements, and result in changing the ellipticity of the light polarization. The PSG takes the unpolarized light from the source and elliptically polarizes it, while the PSG takes the elliptically polarized light reflecting from S and changes its ellipticity. The generalized sample S contains the actual specimen, but also any perturbations on the light polarization (such as vacuum chamber windows) between the specimen and the PSD or after the specimen and before the PSD.

Since the PSG, S, and PSD are not in general ideal, we must take into account the possibility that each of these elements are depolarizing; therefore, the Stokes representation of polarized light must be used. In this case, the Stokes vector is defined as [2].

$$\mathbf{S} = \begin{bmatrix} S_0 \\ S_1 \\ S_2 \\ S_3 \end{bmatrix} = \begin{bmatrix} I_{total} \\ I_x - I_y \\ I_{\pi/4} - L_{\pi/4} \\ I_r - I_l \end{bmatrix} \tag{1}$$

The elements of the Stokes vector are all intensities, and therefore real. The S_0 term is the total intensity, S_1 is the intensity difference of the light polarized in the x-direction minus that in the y-direction, S_2 is the intensity difference of the light polarized in the +45° direction minus that in the –45° direction, and S_3 is the intensity difference of right circular polarized light minus left circular polarized light. If the light beam is totally polarized, then

$$S_0 = (S_1^2 + S_2^2 + S_3^2)^{1/2}. \tag{2}$$

If the light beam is linearly polarized, then $S_3=0$; elliptically polarized light will have $S_3 \neq 0$.

Since the polarization of the input and exit light beam is expressed in terms of Stokes vectors, the generalized sample matrix is a 4×4 Mueller matrix, which consists of real numbers. For the case of an isotropic sample with no polarization-perturbing optical elements, the Mueller matrix is simply [2].

$$\mathbf{M} = \begin{bmatrix} m_{00} & m_{01} & m_{02} & m_{03} \\ m_{10} & m_{11} & m_{12} & m_{13} \\ m_{20} & m_{21} & m_{22} & m_{23} \\ m_{30} & m_{31} & m_{32} & m_{33} \end{bmatrix} = \begin{bmatrix} 1 & -N & 0 & 0 \\ -N & 1 & 0 & 0 \\ 0 & 0 & C & S \\ 0 & 0 & -S & C \end{bmatrix}, \tag{3}$$

where the parameters N, S, and C will be defined later. Perturbations due to windows and other optical elements between the PSG and the specimen, and between the Specimen and the PSD can be incorporated into the generalized sample Mueller matrix by pre- and post- multiplying **M** with a correction matrix.

The intensity of the light reaching the detector is given by

$$I = \mathbf{PSD} \cdot \mathbf{M} \cdot \mathbf{PSG}\ , \tag{4}$$

where **PSD** is the row vector representing the change in light polarization due to the PSD and **PSG** is the column vector representing polarization created by the PSG.

We can see immediately the limitations of ellipsometers based only on linear polarization optical elements. If both the PSG and the PSD contain no compensating optical elements, then only linearly polarized light is generated and detected; therefore $S_3 = 0$ for both the PSG and the PSD and neither the 4th row or 4th column of the sample Mueller matrix is accessible to measurement and the intensity of light

incident upon the detector is not a function of the S parameter. On the other hand, if either the PSG or the PSD contains a compensating optical element (such as a quarter wave plate or a photoelastic modulator), then either the 4th row or 4th column of the sample Mueller matrix is now accessible to measurement and the S parameter may be determined. If the PSD measures both polarizations (such as with the 2-channel spectroscopic polarization modulation ellipsometer [5]) then N, S, and C can be measured simultaneously.

Most SE instruments vary the polarization state as a function of time. For example, a rotating polarizer instrument will have as its PSG and PSD vectors

$$\mathbf{PSG} = \begin{bmatrix} 1 \\ \cos(2\omega t) \\ \sin(2\omega t) \\ 0 \end{bmatrix} \qquad \mathbf{PSD} = \begin{bmatrix} 1 & \cos(2\theta_a) & \sin(2\theta_a) & 0 \end{bmatrix} \tag{5}$$

This results in the intensity reaching the detector being given by

$$I = 1 - N\cos(2\theta_a) + \cos(2\omega t)\,(\cos(2\theta_a) - N) + \sin(2\omega t)\, C \sin(2\theta_a)\,. \tag{6}$$

The interesting sample parameters measured are N and C, and are given as Fourier coefficients of the intensity; the S term is not included in the intensity. Similar expressions can easily be obtained for many other ellipsometers.

The important result of this is that the measured quantities from most spectroscopic ellipsometers are Fourier coefficients, which then can be related to elements of the sample Mueller matrix (N, S, and C for isotropic samples). In general, any ellipsometry experiment measures elements of the sample Mueller matrix **S**, or linear combinations of these elements.

It is always possible to relate calculated Fresnel Reflection Coefficients (FRCs) to elements of the sample Mueller matrix [6] by

$$\mathbf{M} = \mathbf{A} \cdot (\mathbf{J} \otimes \mathbf{J}^*) \cdot \mathbf{A}^{-1}, \tag{6}$$

where

$$\mathbf{A} = \begin{pmatrix} 1 & 0 & 0 & 1 \\ 0 & 0 & 0 & -1 \\ 0 & 1 & 1 & 0 \\ 0 & -i & i & 0 \end{pmatrix}, \quad \mathbf{J} = \begin{pmatrix} r_{pp} & r_{ps} \\ r_{sp} & r_{ss} \end{pmatrix}. \tag{7a,7b}$$

The elements of the **J** matrix are the complex FRCs for light polarized in the indicated direction [p (s) is for light polarized parallel (perpendicular) to the plane of incidence]; $\mathbf{J}^*$ represents the complex conjugate of **J** and $\otimes$ represents the Kronecker product. If the sample is isotropic, then the off-diagonal elements r_{sp} and r_{ps} are 0, and the standard sample Mueller matrix sample (see Eq. 3) is obtained, where

$$\rho = r_{pp}/r_{ss} = \tan\psi\, e^{i\Delta} = \gamma e^{i\Delta}. \tag{8a}$$

$$\dot{N} = \cos(2\psi) = (1-\gamma^2) / (1+\gamma^2) \tag{8b}$$

$$S = \sin(2\psi)\sin(\Delta) = 2\gamma\sin(\Delta) / (1+\gamma^2) \tag{8c}$$

$$C = \sin(2\psi)\cos(\Delta) = 2\gamma\cos(\Delta) / (1+\gamma^2) \tag{8d}$$

As can be seen, $N^2 + S^2 + C^2 = \beta^2 = 1$.

If the sample under investigation is anisotropic (i.e., when the refractive indices of the material now depend upon the direction in the material), then the off-diagonal elements of the sample Jones matrix are not generally 0, and the entire sample Mueller matrix can become populated with non-zero elements, many of which are correlated. If certain symmetry conditions are met (such as that the optic axis is in the plane of incidence or perpendicular to it) [2,7], then $r_{sp} = r_{ps} = 0$, and the sample Mueller matrix will remain block diagonal. Furthermore, the notation that has been developed for isotropic systems must be extended for anisotropic systems. A convenient notation, based on Eqs. 8 above, is given by:

$$\rho = r_{pp}/r_{ss} = \tan\psi\, e^{i\Delta} = \gamma e^{i\Delta}. \tag{9a}$$

$$\rho_{ps} = r_{ps}/r_{ss} = \tan\psi_{ps}\, e^{i\Delta ps} = \gamma_{ps} e^{i\Delta ps}. \tag{9b}$$

$$\rho_{sp} = r_{sp}/r_{ss} = \tan\psi_{sp}\, e^{i\Delta sp} = \gamma_{sp} e^{i\Delta sp}. \tag{9c}$$

$$D = (1+\gamma^2+\gamma_{ps}^2+\gamma_{sp}^2) = 2\,/\,(1+N) \tag{9d}$$

$$N = (1-\gamma^2-\gamma_{ps}^2-\gamma_{sp}^2)\,/\,D \tag{9e}$$

$$S = 2\gamma\sin(\Delta)\,/D \tag{9f}$$

$$C = 2\gamma\cos(\Delta)\,/D \tag{9g}$$

$$S_{ps} = 2\gamma_{ps}\sin(\Delta_{ps})\,/\,D \tag{9h}$$

$$C_{ps} = 2\gamma_{ps}\cos(\Delta_{ps})\,/\,D \tag{9i}$$

$$S_{sp} = 2\gamma_{sp}\sin(\Delta_{sp})\,/\,D \tag{9j}$$

$$C_{sp} = 2\gamma_{sp}\cos(\Delta_{sp})\,/D \tag{9k}$$

Note that $N^2 + S_{pp}^2 + C_{pp}^2 + S_{sp}^2 + C_{sp}^2 + S_{ps}^2 + C_{ps}^2 = 1$. In this case, the sample Mueller matrix becomes

$$\mathbf{M} = \begin{bmatrix} 1 & -N-\alpha_{ps} & C_{sp}+\zeta_1 & S_{sp}+\zeta_2 \\ -N-\alpha_{sp} & 1-\alpha_{ps}-\alpha_{sp} & -C_{sp}+\zeta_1 & -S_{sp}+\zeta_2 \\ C_{ps}+\xi_1 & -C_{ps}+\xi_1 & C+\beta_1 & S+\beta_2 \\ -S_{ps}+\xi_2 & S_{ps}+\xi_2 & -S+\beta_2 & C-\beta_1 \end{bmatrix}, \tag{10}$$

where

$\alpha_{sp} = 2\gamma_{sp}\,/D,$ $\qquad \alpha_{ps} = 2\gamma_{ps}\,/\,D,$

$\beta_1 = (C_{sp}C_{ps} + S_{sp}S_{ps})\,D\,/\,2,$ $\qquad \beta_2 = (S_{sp}C_{ps} - C_{sp}S_{ps})\,D\,/\,2,$

$\zeta_1 = (C\,C_{ps} + S\,S_{ps})\,D\,/\,2,$ $\qquad \zeta_2 = (C\,S_{ps} - S\,C_{ps})\,D\,/\,2,$

$\xi_1 = (C\,C_{sp} + S\,S_{sp})\,D\,/\,2,$ $\qquad \xi_2 = (C\,S_{sp} - S\,C_{sp})\,D\,/\,2.$

It is always possible to associate an ideal Jones matrix calculated from the FRCs (calculated) with a Mueller matrix (measured); the inverse is not true. For example, if the sample acts as a depolarizer, then this direct association cannot be used. A very simple case of this is when the sample consists of a thin film of non-uniform

thickness over the illuminating spot [8]. In this case, $N^2 + S^2 + C^2 = \beta^2 < 1$ and the distribution of film thicknesses can be determined.

III. Calculation of Fresnel Reflection Coefficients

The calculation of the FRCs from multiple thin films is a well-understood problem, if all the films are isotropic and if there are no depolarization effects. The most general method of performing this calculation is due to Abelès [9]. In this formulation, one defines s- and p-transfer matrices for each layer j, given by

$$\mathbf{P}_{j,p} = \begin{pmatrix} \cos b_j & i \sin b_j \cos \phi_j / \tilde{n}_j \\ i \sin b_j \tilde{n}_j / \cos \phi_j & \cos b_j \end{pmatrix}, \quad (11a)$$

$$\mathbf{P}_{j,s} = \begin{pmatrix} \cos b_j & i \sin b_j / \tilde{n}_j \cos \phi_j \\ i \sin b_j \tilde{n}_j \cos \phi_j & \cos b_j \end{pmatrix}, \quad (11b)$$

where $b_j = 2 \pi d_j \tilde{n}_j \cos \phi_j / \lambda$, d_j is the thickness, $\tilde{n}_j$ is the complex refractive index, ϕ_j is the complex angle of incidence, all in the jth layer, and λ is the wavelength of light. The characteristic matrix for the entire layer stack is given by

$$\mathbf{P}_p = \Pi \mathbf{P}_{j,p} \text{ and } \mathbf{P}_s = \Pi \mathbf{P}_{j,s} . \quad (11c)$$

The FRCs for the total structure are then calculated using

$$r_p = (A_p \tilde{n}_0 \cos \phi_0 - B_p) / (A_p \tilde{n}_0 \cos \phi_0 + B_p), \quad (11d)$$

$$r_s = (A_s \cos \phi_0 / \tilde{n}_0 - B_s) / (A_s \cos \phi_0 / \tilde{n}_0 + B_s), \quad (11e)$$

where

$$A_p = (\mathbf{P}_{11,p} + \mathbf{P}_{12,p} \tilde{n}_{sub} \cos \phi_{sub}), \quad (11f)$$

$$B_p = (\mathbf{P}_{21,p} + \mathbf{P}_{22,p} \tilde{n}_{sub} \cos \phi_{sub}), \quad (11g)$$

$$A_s = (\mathbf{P}_{11,s} + \mathbf{P}_{12,s} \tilde{n}_{sub} \cos \phi_{sub}), \quad (11h)$$

$$B_s = (\mathbf{P}_{21,s} + \mathbf{P}_{22,s} \tilde{n}_{sub} \cos \phi_{sub}) . \quad (11i)$$

The subscript 0 refers to the ambient, while the subscript sub refers to the substrate.

If any of the films are anisotropic, then in general r_{sp} and r_{ps} are no longer 0 and a more complicated 4×4 matrix formalism [10,11] must be used, where the matrix elements are complex. If $r_{sp} = r_{ps} = 0$, either because the film is isotropic or because of symmetry considerations, then the 4×4 matrices become block-diagonal 2X2 Abelès matrices.

Another complication arises when the refractive indices of each layer are functions of depth. The most general and straight-forward way of calculating the FRCs is to break the layer into many thinner lamella, each with a constant refractive index, and calculate the FRCs from Eqs. 11 above. Although this procedure works in the limit of very thin lamellae, in actuality, the number of layers required is quite large.

In certain circumstances, it is possible to replace many lamella with a few lamella, *if it is assumed that the dielectric function (both real and imaginary part)* is linear with respect to depth. If it is assumed that the dielectric function of the j-th layer is given by

$$\varepsilon_{j+1} = \varepsilon_j + \alpha\, x, \quad 0<x<d_j \,. \tag{12}$$

It can be shown that [3] the Abelès matrices become:

$$\mathbf{P}_{j,p} = \begin{bmatrix} 1 - (\nu_j^2/2)(\eta_j + \alpha d_j\, (\varepsilon_j + \xi)/3) & i\, \nu_j\, (\varepsilon_j + \alpha d_j\, /2) \\ i\, (\nu_j/\varepsilon_j)\, (\eta_j + \alpha d_j\, \xi/2\varepsilon_j) & 1 - (\nu_j^2/2)(\eta_j + \alpha d_j\, (\varepsilon_j + \eta_j\,)/3\, \varepsilon_j) \end{bmatrix}, \tag{13a}$$

$$\mathbf{P}_{j,s} = \begin{bmatrix} 1 - (\nu_j^2/2)(\eta_j + 2\alpha d_j/3) & i\, \nu_j \\ i\, \nu_j\, (\eta_j + \alpha d_j\, /2) & 1 - (\nu_j^2/2)(\eta_j + \alpha d_j/3) \end{bmatrix}. \tag{13b}$$

where $\nu_j = 2\, \pi\, d_j \,/\, \lambda$, $\xi = n_0 \sin \phi_0$, and $\eta_j = \varepsilon_j - \xi$. These calculations are performed to second order in ν_j and first order in αd_j, so the thickness of each lamella must be sufficiently small that second- or third-order terms can be ignored. Other forms of the dielectric function can be calculated using the formalism of Jacobsson [12].

IV. Optical Functions

The third step in the analysis of SE data is to specify the wavelength-dependent optical functions of each of the layers. The simplest and most straightforward way is to assign the spectroscopic dielectric functions for bulk materials that have been previously measured (see for example Ref. 13 and the associated data disk available from the Optical Society of America). These tabulated optical functions are usually very useful for substrates and certain types of thin films. However, the optical functions of thin film materials tend to be different than the optical functions of their bulk counterparts [14], so alternate ways of determining the optical functions of the layers must also be available.

One such parameterization using effective medium approximations (EMA) has been used for many years. In this case, a composite dielectric function is calculated based on optical function spectra either in the data base or otherwise calculated (see below). The effective medium approximation assigns an intermediate dielectric function to a material using the expression

$$(\varepsilon - \varepsilon_H) / (\varepsilon + 2\,\varepsilon_H) = \Sigma\, f_j\, (\varepsilon_j - \varepsilon_H) / (\varepsilon_j + 2\,\varepsilon_H)\,, \tag{14}$$

where ε_H is the dielectric function of the host material and the sum is taken over all constituents.

There are two variations of effective medium approximation (EMA), depending upon the choice of host materials: (1) the Maxwell Garnett (MG EMA) theory [15], where the major component is taken as the host material, and 2) the Bruggeman (B EMA) theory [16], where $\varepsilon = \varepsilon_H$. Because the composite dielectric function is only on the right-hand side for the MG EMA, the calculation of ε is quite straightforward; this theory is most accurate when the material consists of a well-known major constituent, interspersed with small, isolated minority constituents. In the B EMA,

complex ε exists in both the numerator and the denominator for each constituent, complicating the calculation of ε (see Ref. 17 for a technique to avoid branch cut problems for 2 constituent B EMA calculations). The Bruggeman EMA has been successfully used to simulate the optical functions of surface roughness and interface layers.

In many cases, particularly in dealing with thin film materials that are not very well characterized, it is best to parameterize the dielectric functions of the layer. The Lorentz approximation has often been used for this [18,19], and is given by:

$$\tilde{n}^2 = \varepsilon = 1 + \Sigma A_j \lambda^2 / (\lambda^2 - \lambda_o^2 + i\Gamma\lambda). \quad (15)$$

where the sum goes from 1 to N_L; often one term is sufficient.

There are other parameterizations that have recently been utilized, particularly for approximating the optical functions of amorphous materials. One, based on a calculation of Forouhi and Bloomer (F&B) [20], has received some attention, but is flawed by the assumption that $k(E)>0$ for $E<E_g$, where E_g is the band gap of the amorphous semiconductor; the F&B approximation also is incorrect in the limits as $E \to 0$ (for metals), and as $E \to \infty$, and the Kramers-Kronig determination of the real part is incorrect. A more realistic model [21] is given by

$$\varepsilon_2(E) = A (E - E_g)^2 / E [(E^2 - E_o^2)^2 + \Gamma^2 E^2] \quad E>E_g \quad (16)$$

$$\varepsilon_2(E) = 0 \quad E<E_g .$$

The real part of the dielectric function is calculated from $\varepsilon_2(E)$ using Kramers-Kronig analysis, and results in a closed form. This formulation has several advantages over the F&B calculation: 1) $\varepsilon_2(E) = 0$ below the band gap; 2) $\varepsilon_2(E) \to \text{const}/E^3$ as $E \to \infty$; $\varepsilon_2(E) \to$ constant for F&B; 3) If $E_g=0$, then $\varepsilon_2(E) \to \text{const}/E$ as $E \to 0$; $\varepsilon_2(E) \to \text{const } E$ for F&B. Equation 16 and its Kramers-Kronig transform have been fit to several data sets

found in Refs. 13, resulting in far better fits than found from equivalent fits to the F&B expression.

There are several other ways in which real situations in thin films can be parameterized. The effects of strain on the dielectric functions of materials can be parameterized if reasonably accurate spectroscopic values of the stress-optic constants of the materials are available; these functions are not readily available for many materials, but are available for Si, Ge, and GaAs [22]. Free carrier effects can be included by adding a Drude term to the dielectric function of a layer [23]. If the thin film consists primarily of polycrystalline material, then the optical functions of the film are significantly different from the dielectric functions of the single crystalline material or its amorphous analog (see ref. 24 for the dielectric functions of various forms of silicon); crystallite size effects have been successfully parameterized [23] for very thin, small-grained aluminum films.

V. Comparison of Calculations and Data

The final step in the process to analyze SE data is to compare the measured parameters with calculated parameters. This is a critical step, but has been discussed previously in Refs. 3 and 25; therefore, only a summary will be given here.

It is extremely important to choose a proper figure of merit (FOM) function to use as a comparison between the measured calculated parameters. The most common FOM used [26,27] is the reduced χ^2, which is given by

$$\chi^2 = [1/(n-m-1)] \Sigma [\rho_{exp}(\lambda_i) - \rho_{calc}(\lambda_i,\mathbf{z})]^2/\delta\rho(\lambda_i)^2 , \qquad (17)$$

where n is the total number of data points, m is the number of fitted parameters, $\rho_{exp}(\lambda_i)$ is the experimental data at wavelength λ_i, $\rho_{calc}(\lambda_i,\mathbf{z})$ is the calculated quantity associated with the experimental data at wavelength λ_i and for the parameter vector $\mathbf{z}$ (with m elements), and $\delta\rho(\lambda_i)$ is the error associated with each of

the experimental data points. The errors in the data points will have a random component, which is usually small, and a systematic part, due to errors in the angle of incidence, the natural spread in wavelength due to the monochromator, errors in the wavelength due to the monochromator, errors in the azimuthal angles of the optical elements, etc.

The use of χ^2 as the FOM has several advantages:

(1) It is automatically a measure of the "Goodness of Fit." If $\chi^2 \sim 1$, then the calculated model fits the data; if $\chi^2 >> 1$, the model does not fit the data. If $\chi^2 << 1$ for too many cases, then the error limits have probably been set too large.

(2) The more accurate experimental data points are automatically weighted more than the inaccurate data points. This is particularly important for many rotating element ellipsometers, where measurements of Δ become very inaccurate as $\Delta \sim 0°$ or $\sim 180°$.

(3) If a conversion algorithm such as Levenberg-Marquardt is used, then elements of the calculation can be used to determine error limits of the parameter vector **z**.

Once a FOM is chosen, then one must "guess" at appropriate values of the parameter vector **z**, and converge onto the best fit values of **z** using a conversion algorithm such as Levenberg-Marquardt. This calculation produces the curvature matrix [26,27], given by

$$\mathbf{A}_{i,j} = \partial^2 \chi^2 / \partial z_i \partial z_j \,. \qquad (18)$$

If $\mathbf{E} = \mathbf{A}^{-1}$, then $\delta z_{i,corr} = (E_{ii})^{1/2}$ and $\delta z_{i,uncorr} = (1/A_{ii})^{1/2}$, where $\delta z_{i,corr}$ and $\delta z_{i,uncorr}$ are the correlated and uncorrelated error limits of the ith element of the parameter vector **z** . In addition, the off-diagonal elements of the **E** matrix can be used to calculate the cross-correlation coefficients: $E_{i,j} \,/\, (E_{i,i}\, E_{j,j})^{1/2}$, which can be used to measure correlations between parameters.

In reality, one cannot rigorously define error limits to the fitted parameters if there is any correlation between the fitted parameters [26,27]; all one can do is to define a (m-1)-dimensional ellipsoid which define the confidence limits of each of the fitted parameters. If the fitted function is non-linear (as it is for SE), then the confidence limits are not even described by ellipsoids, but rather a more complicated (m-1)-dimensional surface [26]; however, it often is a good approximation to assume that the confidence limit surfaces are ellipsoidal.

As an example, consider the case of several thicknesses of SiO_2 grown on Si. The complex ρ function was calculated for 4 different SiO_2 thicknesses from 1.5 to 5.3 eV using literature values of the dielectric functions for SiO_2 (ref. 13) and for Si (Ref. 28), assuming an angle of incidence of 65°; errors in ρ were approximated using the procedure described in Ref. 25. These calculated ρ spectra where then fit to a 3 material model, consisting of air/SiO_2/c-Si, where the optical functions of SiO_2 are parameterized using Eq. 15 and assuming that λ_1=92.3 nm and Γ=0. This model consists of 2 fitable parameters: the SiO_2 thickness, and the Lorentz parameter A. The results are summarized in Table I. Since m=2 for this case, the resulting confidence interval ellipsoids are just an ellipses, and are plotted in Fig. 2. The results shown in Table I and Fig. 2 are related: the correlated error is just the total height of the error ellipse along the direction of interest, while the uncorrelated error is the height of the ellipse at 0 error for the other parameter.

As can be seen From Table I and Fig. 2, very thin films result in large uncertainties in the fitted parameters, and there is a large correlation between the two parameters. As the film gets thicker, both the correlated and uncorrelated error in A is decreased considerably; the absolute error in d also decreases modestly, but the relative error decreases considerably. This example quantifies what has been known for some time: it is not possible to determine both the film thickness and the optical functions of a very thin film.

VI. Summary

In this paper, we have looked at the analysis of spectroscopic ellipsometry data in detail to determine the elements of the calculation. There are 4:

(1) Determination of the measured parameters.

(2) Specification of the surface model.

(3) Determination of the optical functions of the constituent films and substrate.

(4) Parameterization of the model and the fitting of the data with calculated spectra.

Each of these steps is important, but step 4 is particularly important; if a "goodness of fit" parameter is not calculated, then the researcher is relying on "chi-by-eye" [26], and therefore has no quantifiable measure of whether or not his model fits the data.

This research was sponsored by the Division of Materials Science, Oak Ridge National Laboratory, managed by Lockheed Martin Energy Research, for the U.S. Department of Energy, under contract DE-AC05-96OR22464.

References

1. Spectroscopic Ellipsometry, *Thin Solid Films*, **233** (1993) 234 .
2. R. M. A. Azzam and N. M. Bashara, *Ellipsometry and Polarized Light,* North Holland, Amsterdam, 1977.
3. G. E. Jellison, Jr., *Thin Solid Films* , **233** (1993) 416.
4. P. S. Hauge, *Surf. Sci.* , **96** (1980) 108.
5. G. E. Jellison, Jr. and F. A. Modine, *Appl. Opt.*, **29** (1990) 959.
6. R. Barakat, *Opt. Commun.* **38** (1981) 159; C. Brosseau, C. R. Givens, and J. M. Kwiatkowski, *J. Opt. Soc. Am.*, **10** (1993) 2248.
7. H. Wöhler, G. Haas, M. Fritsch, and D. A. Mlynski, *J. Opt. Soc. Am., A* **8** (1991) 536.
8. G. E. Jellison, Jr. and J. W. McCamy, *Appl. Phys. Lett.* , **61** (1992) 512.
9. F. Abelès, *Ann. de Physique,* **5** (1950) 596.
10. S. Teitler and B. Henvis, *J. Opt. Soc. Am.*, **60** (1970) 830.
11. D. W. Berreman, *J. Opt. Soc. Am.*, **72** (1972) 502.
12. R. Jacobsson, in E. Wolf (ed.) *Progress in Optics*, 5, Wiley, 1965, p. 247.
13. E. Palik (ed.), *Handbook of optical constants of solids,* Academic Press, Orlando, 1985; *Handbook of optical constants of solids, II* Academic Press, Boston, 1991.
14. G. E. Jellison, Jr., L. A. Boatner, D. H. Lowndes, R. A. McKee, and M. Godbole, *Appl. Opt.*, **33** (1994) 6053.
15. J. C. Maxwell Garnett, *Philos. Trans. R. Soc. London, 203* (1904) 385; *A 205* (1906) 237.
16. D. A. G. Bruggeman, *Ann. Phys., (Leipzig)* **24** (1935) 636.
17. Ph. J. Roussel, J. Vanhellemont and H. E. Maes, *Thin Solid Films,* **234** (1993) 423.

18. G. E. Jellison, Jr. *J. Appl. Phys.* , **69** (1991) 7627.

19. S. Y. Kim and K. Vedam, *Thin Solid Films,* **166** (1988) 325.
K. Vedam and S. Y. Kim, *Appl. Opt.* **28** (1989) 2691.

20. A. R. Forouhi and I. Bloomer, *Phys. Rev. B***34** (1986) 7018.

21. G. E. Jellison, Jr. MS in preparation.

22. P. Etchegoin, J. Kircher, M. Cardona, and C. Grein, *Phys. Rev. B***45**(1992) 11721;
P. Etchegoin, J. Kircher, and M. Cardona, *Phys. Rev. B***47** (1993) 10292;
P. Etchegoin, J. Kircher, M. Cardona, C. Grein, and E. Burstarret, *Phys. Rev. B*4XX199x) xxxxx

23. H. V. Nguyen, I. An, and R. W. Collins, *Phys. Rev. Lett.* ,**68** (1992) 994; *Phys. Rev. B*, **47** (1993) 3947.

24. G. E. Jellison, Jr., M. F. Chisholm, and S. M. Gorbatkin, *Appl. Phys. Lett.,* **62** (1993) 3348.

25. G. E. Jellison, Jr., *Appl. Opt.* , **30** (1991) 3354.

26. W. H. Press, B. P. Flannery, S. Al Teukolsky and W. T. Vettering, *Numerical Recipes, Second Edition,* Cambridge, University Press, 1992.

27. N. R. Draper and H. Smith, *Applied Regression Analysis,* Wiley, New York, 1981.

28. G. E. Jellison, Jr., *Optical Materials,* **1** (1992) 41.

Table I

The results of confidence limits to the calculation described in the text. The quantity d_{SiO2} is the the SiO_2 film thickness, with correlated and uncorrelated errors shown as δd_{corr} and δd_{uncorr} respectively. The quantity A=1.099 for all calculations, but the orrelated and uncorrelated errors δA_{corr} and δA_{uncorr} vary considerably with film thickness.

d_{SiO2} (nm)	δd_{corr} (nm)	δd_{uncorr} (nm)	δA_{corr}	δA_{uncorr}	Cross-correlation
10	0.54	0.11	0.138	0.027	-0.981
20	0.40	0.12	0.041	0.012	-0.955
50	0.18	0.12	0.006	0.004	-0.727
100	0.25	0.15	0.004	0.003	-0.788

Figure Captions

1. A schematic of a generalized ellipsometer. The PSG is the polarization state generator, the PSD is the polarization state detector, and the S is the generalized sample, which contains all elements between the PSG and the PSD, including windows.

2. The confidence limit ellipses for the 2-parameter example described in the text. The correlated and uncorrelated errors are tabulated in Table I.

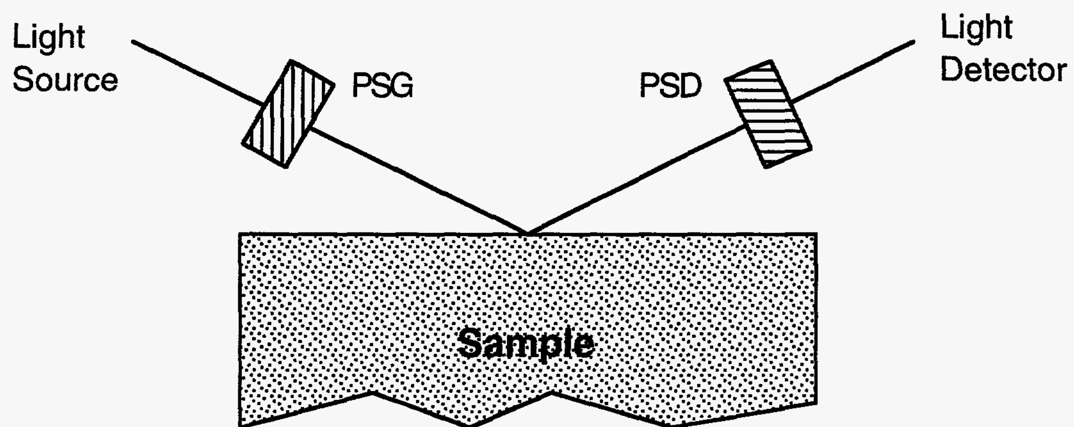

Figure 1

G. E. Jellison, Jr.
Oak Ridge National Lab
PO box 2008
Oak Ridge, TN 37831-6056
423-576-7309

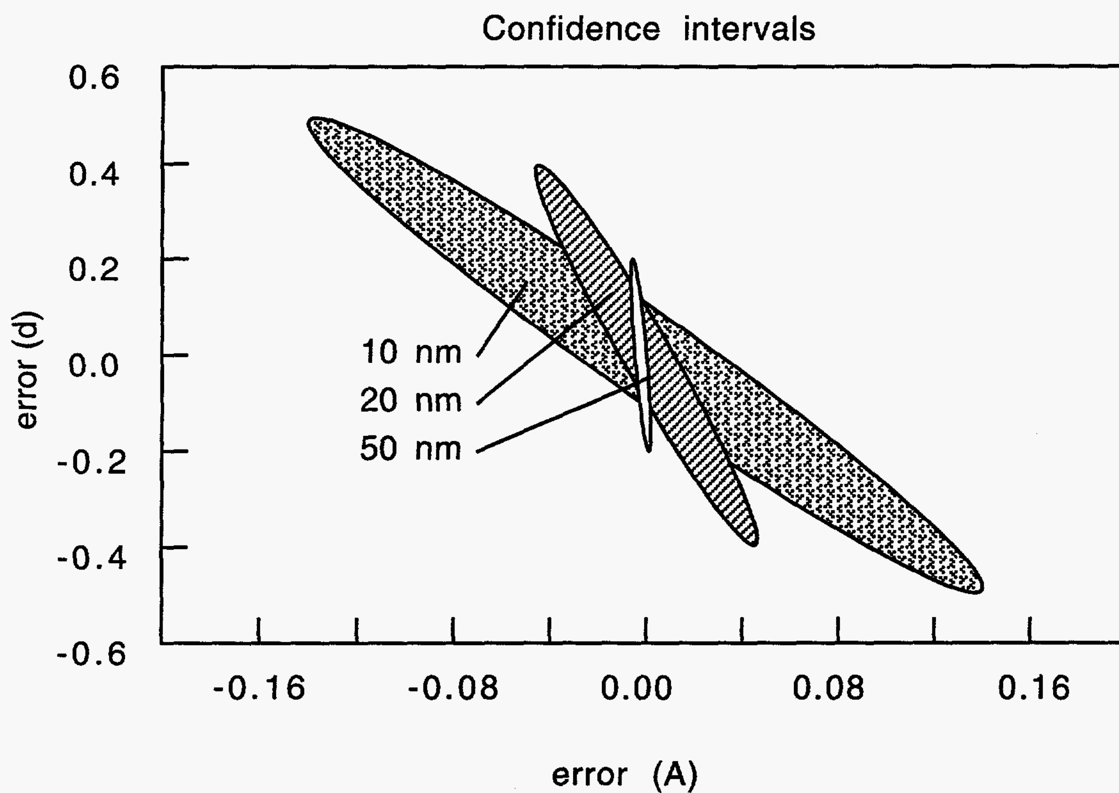

Figure 2

Jellison
Oak Ridge National Lab.
PO Box 2008
Oak Ridge, Tn 37831-6030
423-576-7309